SHOP: Receptor-Based Scaffold HOPping by GRID-Based Similarity Searches

Rikke Bergmann,*,† Tommy Liljefors,† Morten D. Sørensen,‡ and Ismael Zamora§,||

Department of Medicinal Chemistry, Faculty of Pharmaceutical Sciences, University of Copenhagen, Universitetsparken 2, DK-2100 Copenhagen Ø, Denmark, LEO Pharma A/S, Industriparken 55, 2750 Ballerup, Denmark, Lead Molecular Design, Valles 96-102, Loc 27, 08172 Sant Cugat de Valles, Barcelona, Spain, and Grup de Recerca Biomédica- IMIM Universitat Pompeu Fabra, Aiguader, 80 08124 Barcelona, Spain

Received October 23, 2008

A new field-derived 3D method for receptor-based scaffold hopping, implemented in the software SHOP, is presented. Information from a protein−ligand complex is utilized to substitute a fragment of the ligand with another fragment from a database of synthetically accessible scaffolds. A GRID-based interaction profile of the receptor and geometrical descriptions of a ligand scaffold are used to obtain new scaffolds with different structural features and are able to replace the original scaffold in the protein−ligand complex. An enrichment study was successfully performed verifying the ability of SHOP to find known active CDK2 scaffolds in a database. Additionally, SHOP was used for suggesting new inhibitors of p38 MAP kinase. Four p38 complexes were used to perform six scaffold searches. Several new scaffolds were suggested, and the resulting compounds were successfully docked into the query proteins.

INTRODUCTION

Structure-based methods for the design of new lead structures are used routinely within drug discovery. These methods include docking based virtual screening where large compound libraries are screened, and compounds are selected based on how well they fit into a receptor judged by their nonbonded interactions and an estimation of their binding affinities.[1−4] Receptor-based pharmacophore development where chemical properties of a receptor are condensed into pharmacophoric features connected by distance and angle constraints and used to search a compound database is another well-established method. In situations where the structure of the binding site is not available ligand-based pharmacophores can be used.[5] De novo design is yet another structure based approach where molecular fragments are fitted into a receptor and joined by linkers forming an entirely new molecule.[6−10]

The methods described above all focus on finding entire molecules which fit into a known receptor and are suitable for finding new leads. When a lead is already available, but inappropriate for reasons such as intellectual property rights, ADME/Tox, selectivity, or affinity, a possibility is to change just a fragment of the lead compound with another structurally different fragment that can interact with the same part of a receptor, retaining the remaining parts of the molecule. This approach is called scaffold hopping. Several ligand-based scaffold hopping methods have now been developed and only a few protein structure-based scaffold hopping methods.[11−23]

We recently reported a new ligand-based scaffold hopping method, SHOP, based on GRID[24,25] derived descriptors,[21] where the scaffolds are retrieved from a database based on their geometrical properties, shape, and interaction possibilities and subsequently ranked according to how well they can substitute the query scaffold. Ligand-based SHOP is intended for cases where known ligands exist but no structural information of the receptor is available. The advantage is that new scaffolds can be found that are structurally unrelated to the query scaffold but can interact similarly with the receptor. The disadvantage is that additional interactions between the receptor and the new scaffolds cannot be expected to occur because the receptor is unknown. When the protein structure is accessible, it would be desirable to take advantage of the abundant information that can be obtained from the binding site, and for this purpose a new SHOP-based approach, receptor-based scaffold hopping, was developed and is described in this paper. In receptor-based SHOP, the full interaction profile of the receptor is taken into account when finding and scoring scaffolds. The advantage of exploring the interaction possibilities of the receptor for scaffold hopping is an increased probability of finding scaffolds that provide new interactions with the receptor while having an entirely different structural composition. A protein−ligand complex must be available as a starting point. The complex is described by geometrical descriptors of the scaffold binding site as well as a 3D interaction energy map of the binding site computed by GRID using five different chemical probes. The scaffolds in the database to be searched are described geometrically as well as by atom-pair descriptions of atom types to be fitted onto the GRID computed map. This allows for a ranking of scaffolds in a database according to how well they fit into the scaffold binding site.

* Corresponding author phone: + 45 35 33 64 06; fax: + 45 35 33 60 40; e-mail: rb@farma.ku.dk.
† University of Copenhagen.
‡ LEO Pharma A/S.
§ Lead Molecular Design.
|| IMIM Universitat Pompeu Fabra.

10.1021/ci800391v CCC: $40.75
Published on Web 03/05/2009

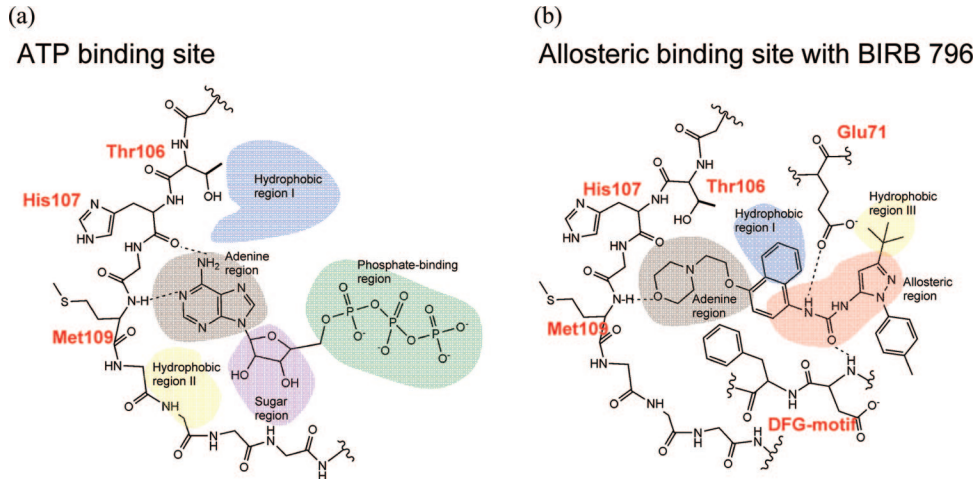

Figure 1. The binding site of p38 MAP kinase can be divided into a number of subsites. The sites of two known conformations of the p38 MAP kinase active site are illustrated. (a) The ATP binding site is known from other kinases such as CDK2, MEK1, and MEK2 and adapted from these. The ATP binding site has classically been divided into five regions: the adenine region where a crucial hydrogen bond is formed to the hinge Met109, the sugar region where the ribose motif binds, the phosphate-binding region where the triphosphate motif binds, and the hydrophobic pockets I and II that confer selectivity and increased affinity to p38 ligands. (b) In addition to the adenine region and the hydrophobic pocket I, the allosteric site contains an allosteric region and the hydrophobic pocket III.

In order to test the approach, we carried out a study of receptor-based scaffold hopping using p38 MAP kinase (p38). This kinase, which is involved in inflammatory and autoimmune diseases, was selected as a model system based on the vast amount of structural information available and the fact that it is an interesting pharmaceutical target. It offers a varied binding site including several hydrophobic pockets and numerous hydrogen bonding possibilities including the crucial hydrogen bond donor Met109 as well as the potential for charged interactions. Furthermore, the binding site is composed of both buried and solvent exposed regions (Figure 1). Two different conformations of the binding site are used in this study: the conformation to which ATP binds and an allosteric conformation where the activation loop has undergone a large conformational change.[26] Figure 1a illustrates the ATP binding site. Although no crystal structure has been reported with ATP complexed to p38, the binding mode has been proposed from the known binding mode in other kinases such as CDK2, MEK1, and MEK2.[27,28] Figure 1b illustrates the allosteric binding site as exemplified with the allosteric inhibitor BIRB 796.[26]

METHODS

SHOP Methodology. In receptor-based SHOP v. 1.0, scaffold hopping is performed by describing and comparing a protein binding site and scaffolds in a database in terms of several GRID derived descriptors. The binding site definition starts by selecting a fragment from a protein-bound ligand to be replaced with a fragment from a selected database. The selected fragment, in the following termed the query scaffold, is removed from the binding site. The query scaffold is used to indicate the geometry of the attachment points of the scaffold to the remaining parts of the ligand as well as to define the binding pocket for the receptor interaction profile computation. Positions on the query scaffold where the remaining components of the ligand were attached (reactive sites) are designated 'anchor points'. These substituents will be reattached to the new scaffolds retrieved from the database. The anchor points are used for the calculation of all descriptors (see details below). Distances and dihedral angles for the binding site description are measured between anchor points of the query scaffold. GRID molecular interaction fields (MIFs)[25] are calculated within a box shaped region defined by the removed scaffold. Since the GRID computation is done in a regular box, grid points at the corners of the box could be outside the region of interest. These are removed leaving a volume defined by a customizable cut out distance to the query scaffold structure. The points inside the volume defined by the query scaffold and the cut out distance are the ones used in the following calculation. The scaffolds in the database are described geometrically by distances and dihedral angles as was described above for the query scaffold, and the interaction profile is obtained by converting all atoms into GRID probe atom types which can be matched onto the MIF in the binding site. A similarity index calculation is then performed assigning a value between zero and one to each scaffold which indicates how well it could substitute the query scaffold. A ranked database is produced placing the scaffolds that best fit into the receptor at the top of the list. Finally, the database scaffolds are aligned to the query scaffold using the anchor points and greatest vdW volume overlap.

SHOP DETAILS

Receptor Description. Three types of descriptors are used to describe the receptor: (a) the distance between anchor points of the query scaffold, (b) the dihedral angle between the anchor points and their connecting points on the query scaffold, and, finally, (c) a GRID derived molecular interaction profile of the receptor related to the GRIND descriptors.[29,30]

a) The distance between anchor points is measured in Å and recorded as a presence versus distance bin representation (Figure 2a). The presence of a specific distance between two anchor points is depicted as a value of one, while the absence is recorded as a zero-value. A minor overlap between bins is allowed by describing the distances by Gaussian functions. The Gaussian distributions have maximum probability on the distance measured and 50% probability at ±0.5 Å from the measured distance. The number of bins is fixed to 100, and the bin interval is set to 0.8 times the grid step of the

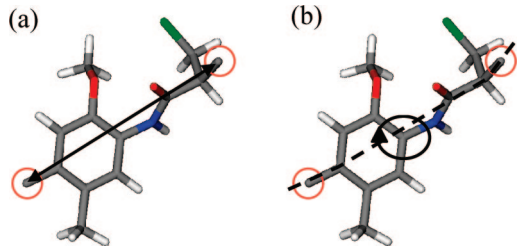

Figure 2. Geometric descriptors: (a) the distance between anchor points and (b) the dihedral angle between anchor points and their connecting atoms. Anchor points are illustrated with red circles.

MIF calculations which is 0.5 Å. Thus, the bin interval is $0.8 \times 0.5 = 0.4$ Å.

b) The dihedral angles are by default recorded in bins of 5 degrees. Otherwise the description is done as for the distance with presence or absence of values and Gaussian functions surrounding the present values (Figure 2b).

c) The coordinates of the query scaffold are used to place a grid box inside the protein cavity. By default the size of the grid box exceeds the extremes of the scaffold by 2 Å, and the distance between grid points is 0.5 Å. Five different properties are calculated at each grid point using GRID probes. These are the hydrophobic interactions (DRY), the hydrogen bond donor (N1) and the hydrogen bond acceptor (O) properties, and, finally, the positive (N1+) and negative charges (O−). Only favorable (negative) interaction energies are recorded. The noise is removed by using a cut out procedure originally described for the GOLPE program.[31] This procedure eliminates the MIF beyond a certain cutoff distance from the query scaffold leaving an irregularly shaped volume inside the receptor defined by the scaffold. The default value of the cutoff distance is 1 Å. The distance is then recorded between each anchor point and each of the remaining points of favorable interaction energies and recorded in a correlogram describing the interaction energies as a function of the distances recorded in distance bins of 0.4 Å (Figure 3a-d). The default number of bins is 100, consequently, allowing maximum distances of 40 Å between anchor points and points of favorable interaction. Five correlograms for each anchor point in the query are obtained—one for each calculated interaction property. For a two anchor point scaffold, a total of ten correlograms would describe the protein interaction profile. This descriptor is unique to receptor-based SHOP.

Database Scaffold Description. The scaffolds in the database are described by the distances and the dihedral angles between anchor points as described above. In addition, a novel atom-pair description (d) is employed, where distances between the anchor points and each atom of the scaffold are measured as follows:

d) Each of the atoms in the scaffold is converted into a relevant GRID probe describing the properties of the atom. For example, the carbon atoms in an aromatic ring are converted into DRY probes, and the distances between the anchor points and each "DRY probe" in the molecule are recorded (Figure 3e-g). Similarly, the oxygens of carbonyl groups are converted into O probes, and the distances between each anchor point and the carbonyl oxygens are recorded in an "O-probe" representation. Each anchor point is then described in a fingerprint like manner showing the presence or absence of a distance (one or zero) as a function of the distance in Å (Figure 3h). Similar to the protein interaction profile, the size of the distance bins is 0.4 Å, and the number of bins is 100 ensuring that the number of interaction profile representations per probe is the same as for the receptor. This descriptor was not described in the ligand-based SHOP paper[21] but can be included in SHOP ligand-based scaffold hopping where the description is made for both the query- and database scaffolds and then compared. In receptor-based scaffold hopping, this comparison between query- and database scaffolds is avoided to prevent bias introduced from the query scaffold structure, and instead the interaction possibilities from the surrounding amino acid environment are exclusively used.

Similarity Calculations. The similarity between two scaffolds described by each of the descriptor sets are compared using a modified version of the Carbó index[32] (eq 1)

$$\mathrm{Sim(descriptor)} = \frac{\sum_{i=0}^{bins} X_i^A \times X_i^B}{\sqrt{\sum_{i=0}^{bins} (X_i^A)^2} \times \sqrt{\sum_{i=0}^{bins} (X_i^B)^2}} \quad (1)$$

where X^A and X^B are the numerical values of the description of the query complex A and the database scaffold B. The bins are the number of available distance bins (default is 100). The comparison between interaction profiles of query protein and database scaffolds is shown in eq 2, where "*PROBE*" is one of the five previously defined GRID probes. "*Finger*" is the presence or absence of a certain anchor point-atom type distance (one or zero) in the database scaffolds, and E is the favorable energy of interaction recorded at a given distance from the anchor point inside the receptor.

$$\mathrm{Sim(PROBE)} = \frac{\sum_{i=0}^{bins} Finger_i^{PROBE} \times E_i^{PROBE}}{\sqrt{\sum_{i=0}^{bins} (Finger_i^{PROBE})^2} \times \sqrt{\sum_{i=0}^{bins} (E_i^{PROBE})^2}} \quad (2)$$

The total similarity ($\mathrm{Sim_{tot}}$) is the sum of the similarity values of the seven descriptors (d), the five interaction profile characterizations, the distance, and the dihedral characterization, using individual weights (w) for the similarity indices (eq 3). The default value of all weights is 1.0.

$$\mathrm{Sim_{tot}} = \Sigma \mathrm{w_d Sim(descriptor)} \quad (3)$$

The similarities of all possible alignment combinations are compared, e.g. the comparison of two compounds A and B with two anchor points A1, A2 and B1, B2, would give two possible similarity sums based on alignments (A1;B1+A2;B2) and (A1;B2+A2;B1). The anchor point alignment giving the highest similarity is selected.

Virtual Reaction Utility Program. In the Virtual Reaction utility program of SHOP, 39 different substitution reactions with reactants and products are defined. From the 39 reactions, it is possible to select all or some of them to build a database. Figure 4 shows an example of one of the defined reactions in the database, the Biginelli reaction.[33]

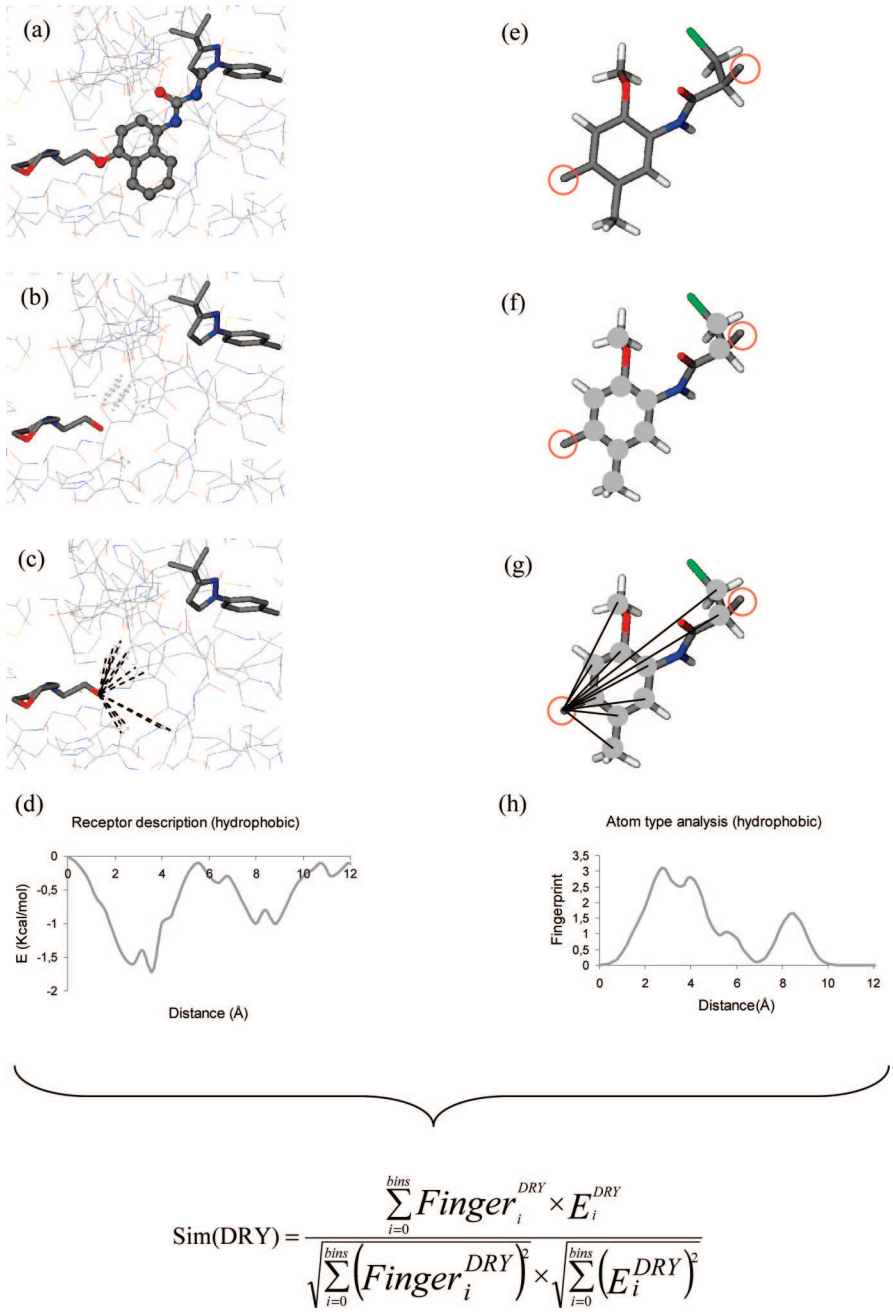

$$\mathrm{Sim(DRY)} = \frac{\sum_{i=0}^{bins} Finger_i^{DRY} \times E_i^{DRY}}{\sqrt{\sum_{i=0}^{bins} \left(Finger_i^{DRY}\right)^2} \times \sqrt{\sum_{i=0}^{bins} \left(E_i^{DRY}\right)^2}}$$

Figure 3. Illustrated are the interaction profile descriptions and comparison of the protein receptor and a database scaffold. (a) The fragment to be substituted is defined and removed within the protein−ligand complex. (b) GRID computations are performed within the receptor with five GRID probes. The DRY probe was used in this illustration. (c) The distances between each anchor point and each point of favorable energy are measured and recorded in a correlogram (d). (e) For the database scaffolds each atom is converted into an appropriate GRID probe (here the hydrophobic DRY is shown), and (f) the distance from each anchor point to each atom of a certain property is measured (g) and recorded (h). Finally, the similarity between the two descriptions is measured (see details in the text). The figure illustrates the description for one anchor point only, but measurements are made for all anchor points.

The reaction is composed of reactive fragments and products substituted with R-groups (Figure 4).

When using the Virtual Reaction Utility Program, a compound file containing reactants must be introduced in 2D SDF format. These could be purchasable or in-house available compounds. Fragment recognition occurs for each of the reactants identifying reactive fragments that theoretically could undergo one or several of the defined reactions. The reactant in Figure 4b contains a urea fragment which has been recognized to be able to participate in the Biginelli reaction (green solid circle).

Associated with each reaction are possible substituents of the reactive fragment. In the example in Figure 4, the reactive urea fragment could be flanked by either alkyl or aromatic substituents. The remaining two building blocks are still unknown except for the fact that one should contain an aldehyde fragment and the other a β-keto ester. The substituents of the urea fragment in the imported reactant file are placed in the positions of the urea R-groups in the reaction products (R4 and R5 in Figure 4 marked by dotted circles). The remaining R-groups (R1, R2, and R3) of the products are converted into anchor points to complete the

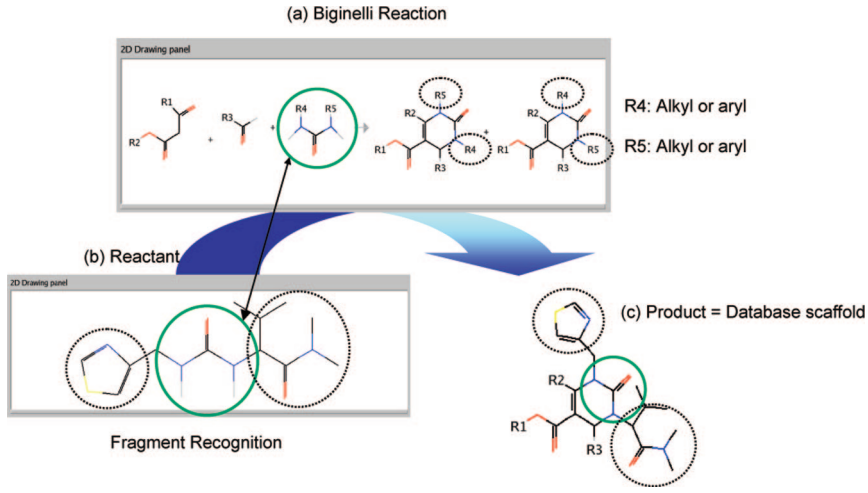

Figure 4. The Virtual Reaction utility program is illustrated here. Reactions are defined by fragments of reactants and products. (a) As an example the Biginelli reaction is illustrated. (b) Fragment recognition of input reactants occurs (encircled in green), and possible reactions where the reactant can take part are identified. (c) The products of the identified reactions are converted into scaffolds for the database by attaching reactant substituents at the appropriate R-group positions of the products (encircled with dotted lines). Finally, the remaining R-group positions are converted into anchor points.

2D scaffolds for the database (Figure 4c). A 2D to 3D molecule conformation generator based on the MM3 force field[34] ensures that product 2D files are converted into one or several 3D conformers.

It is also possible to obtain scaffold databases by attaching anchor points to available compound SDF files. This can be done manually or by using an Anchor definition tool as implemented in the software.

PROCEDURES

Database Generation. The scaffold databases were created with the Virtual Reaction utility program of SHOP allowing all 39 reactions. Building blocks for the reactions were taken from the providers Maybridge and Specs building block libraries[35,36] and imported in 2D SDF format. 2D to 3D conversion and generation of maximum 40 conformations of each new scaffold was done using the molecule conformation generator. The maximum conformational energy allowed was 10 kcal/mol. The scaffolds in the databases contained 1−5 anchor points. The database for the CDK2 scaffold recovery study was built using building blocks from Maybridge and contained 10,556 scaffolds and a total of 124,317 conformers. For recovery purposes, the database was seeded with 47 CDK2 scaffolds in their bioactive conformations extracted from 41 X-ray structures from the RCSB Protein Data Bank (PDB)[37,38] (see below). For the p38 case study, building blocks from Maybridge as well as Specs were included, and the resulting database contained 15,760 scaffolds with a total of 186,618 conformers.

Protein and Ligand Preparations. All computational procedures were performed on a Red Hat Enterprise 3 Linux PC. Molecular modifications were made using Maestro v. 7.5.[39] All X-ray structures are represented by their PDB codes.

PDB files of the protein−ligand complexes were imported into Maestro, and ligands were extracted and inspected manually for corrections of MacroModel atom types and connectivities. Scaffolds were created by removal of the substituents and insertion of dummy atoms as markers for anchor points at the scissile positions. Subsequently, hydrogens were added, and the scaffolds were saved in mol2 format for query purposes. Scaffolds for recovery purposes were imported into the query database in their bioactive conformations.

The query proteins were prepared as follows. Waters were removed from all protein−ligand complexes. Asn/Gln/His protein flips were inspected using Reduce.[40] Only flips within 12 Å from the native ligands were considered. For 1KV2 Asn60, His64, Asn114, and Asp155 were flipped, for 1W7H Asn115 was flipped, and for 1BMK Asp155 was flipped. The query scaffolds were removed from the binding sites and prepared as described above. To prevent the binding regions of the remaining substituents from being occupied by the new scaffolds, the substituents were left in the binding sites prepared for SHOP interaction profile calculations. Finally, the query proteins were saved in PDB format. For docking purposes, hydrogens were added to the proteins, and the substituents were removed from the binding site. The phenol ring of Tyr35 is missing in 1KV2 and was therefore added to the protein−ligand complex. A conformational analysis of the Tyr35 side chain was performed using MacroModel v. 9.0 and the MMFF94 force field, and the conformation with the global energy minimum was inserted into the protein structure. Furthermore, the activation loop (residues 170−184) near the allosteric region of the binding site is missing in 1KV2. The activation loop was modeled using MODELER 6v2 and with the c-Abl kinase as a template (PDB code: 1IEP).[41,42]

CDK2 Scaffold Recovery. Recovery of known CDK2 scaffolds obtained from the RCSB Protein Data Bank was investigated to validate the receptor-based SHOP procedure. The scaffold structures are enclosed as Supporting Information. They all include a fragment that interacts with the hinge Leu83 in the adenine region of the CDK2 via a hydrogen bond but are otherwise varied in size and interactions with the receptor. Eleven scaffolds contain one anchor point, and 29 scaffolds contain two anchor points. The X-ray structures 1GZ8 and 1OGU were used as queries, and the query scaffolds are illustrated in Figure 6. The recovery factors

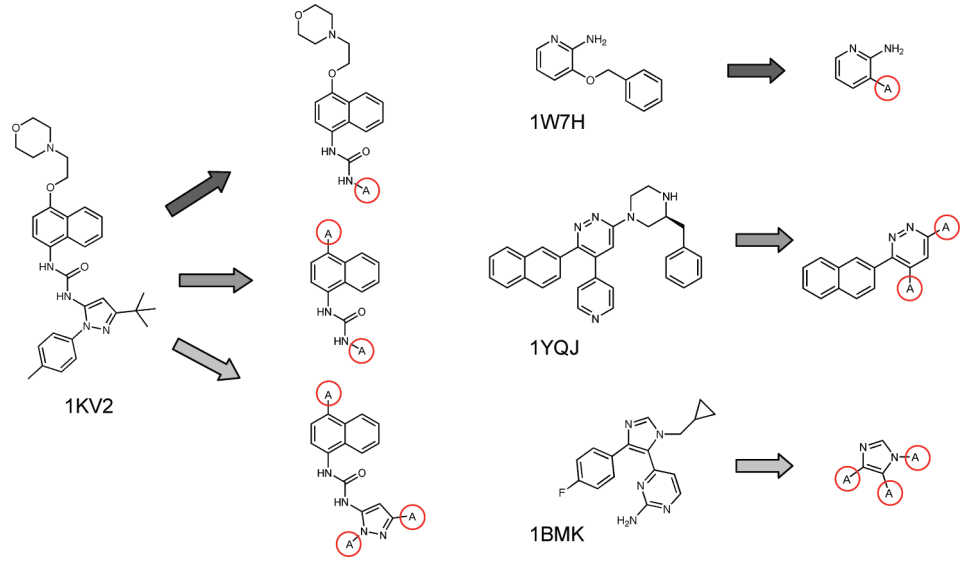

Figure 5. The query scaffolds were constructed from four protein−ligand complexes. The PDB codes are listed below the ligand structures. Three scaffolds were constructed from the 1KV2 crystal structure with one, two, and three anchor points, respectively. From each of the X-ray structures 1W7H, 1YQJ, and 1BMK one scaffold was constructed.

($RF_{\%}$) for the recovery of the known actives in the top fraction of the database were calculated using eq 4

$$RF_{\%} = \frac{KA_{\%}}{NC_{\%}} / \frac{KA_{TOTAL}}{NC_{TOTAL}} \quad (4)$$

where $KA_{\%}$ is the number of known actives recovered in x % of the database, and KA_{TOTAL} is the total number of known actives in the database. NC_{TOTAL} is the total number of compounds in the database, and $NC_{\%}$ is the number of compounds in x % of the database. The recovery at 1%, 2%, and 10% of the database was calculated (Table 1a,b).

Methodology Case Studies. Case studies mimicking real case scaffold hopping scenarios were conducted using four p38 complex structures from the RCSB Protein Data Bank.

One complex (1KV2) including an inhibitor in the allosteric pocket and three complexes (1W7H, 1YQJ, 1BMK) including ATP competitive inhibitors (Figure 5) were used as queries for the searches. The criteria for selecting the query scaffolds were the presence of varying number of anchor points as well as diverse interactions with the receptor. Six different scaffolds were selected (Figure 5). These query complexes were used to search the database for new scaffolds with both 1 Å and 2 Å cutoff distances. A postprocessing procedure was performed for the p38 case studies to exemplify how the scaffolds, resulting from a SHOP search, could be handled. For each search, the top 100 scaffolds were collected, and substituents were attached using a perl script. Subsequently, they were docked into the p38 X-ray structure from which the query was taken. Poses where the substituents had a low rms to their original position and where the Met109 interaction was satisfied were visually inspected. A selected example from each query is illustrated in the Results section. For future studies it could be interesting to compare the results obtained by ligand- and receptor-based SHOP.

Allosteric Inhibitor Query Complex. The p38 complex 1KV2 contains the allosteric inhibitor BIRB 796 (Figures 1 and 5).[26] Three different scaffolds were defined from BIRB 796 with one, two, and three anchor points, respectively (Figure 5). BIRB 796 has interactions in the adenine region with Met109 and in the allosteric site with Glu71 and Asp168 as well as in the hydrophobic pockets I and III.

ATP Competitive Inhibitor Complexes. Three complexes were chosen with ATP competitive inhibitors. One scaffold was defined from each of these with one, two, and three anchor points, respectively (Figure 5).

The 1W7H complex contains the inhibitor 3-(benzyloxy)-pyridin-2-amine (Figure 5).[43] The selected query scaffold contains one anchor point and interacts with the hinge region Met109 and His107 with two hydrogen bonds. Additionally, a dipole−dipole interaction is present between the C═O of Met109 and CH of the pyridyl C6.[43] The retained benzyloxy substituent that will be attached to the new scaffolds interacts in the hydrophobic pocket I.

A two anchor point scaffold was created from the inhibitor (S)-6-(3-benzylpiperazin-1-yl)-3-(naphthalen-2-yl)-4-(pyridin-4-yl)pyridazine (pyridazine inhibitor) of the 1YQJ complex (Figure 5).[44] The selected query scaffold interacts in the hydrophobic pocket I, with the hinge region as well as with Lys53. The retained fragments that will be attached to new scaffolds suggested by SHOP have interactions with Met109, Ser154 and in the hydrophobic pocket II.

The imidazole fragment of the 1BMK[45] inhibitor 4-(1-(cyclopropylmethyl)-4-(4-fluorophenyl)-imidazole-5-yl)pyrimidine-2-amine (SB218655) was selected as a three anchor point query scaffold (Figure 5). The chosen imidazole query scaffold acts as a linker between the three substituents and interacts with a hydrogen bond with Lys53. The substituent has interactions in the hydrophobic pocket I, with the hinge region and with the glycine rich loop in the roof of the binding pocket.

Docking. The top 100 new compounds were prepared for docking using LigPrep v. 2.0[46] to assign protonation states in the pH range 6.4−8.4, to consider tautomerism, and to energy minimize the compounds using the OPLS2005 force field. Subsequently, they were docked into the empty query p38 binding sites using GLIDE XP v. 4.0.[47,48] A maximum of 20 poses per compound were allowed, and otherwise default settings were applied. Only poses with an rmsd ≤ 3 Å of the substituents compared to the native complex were

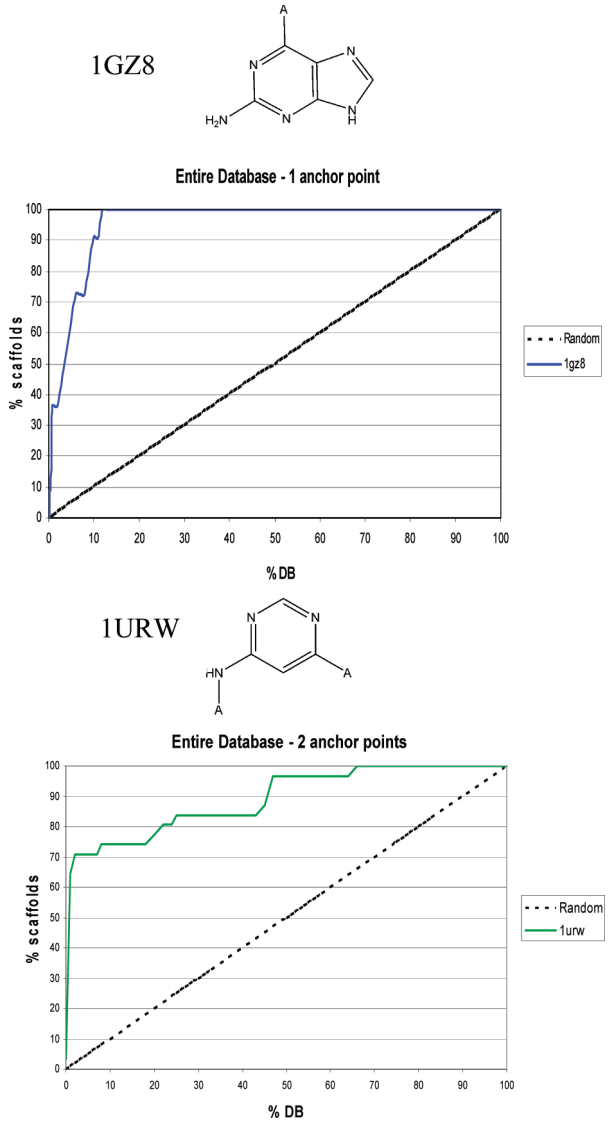

Figure 6. Enrichment curves for recovery of known active CDK2 scaffolds. The curves show the percentage of known CDK2 scaffolds recovered as a function of the investigated fraction of the ranked database. The query scaffolds are illustrated above the curves.

considered. Furthermore, only poses interacting with the hinge Met109 with an energy ≤ −4.0 kcal/mol were considered. This was done using a GRID interaction energy calculation using the POSI directive.[49] The procedure considered each atom position of the docked compound which was converted one by one into a relevant GRID probe such as the DRY probe for an aromatic carbon and the O probe for a carbonyl-oxygen. Then the interaction energy was calculated between the probe and each amino acid in the binding site. Finally, the interaction energies for each atom of the bound ligand were summed up and recorded for each amino acid in the binding site. When comparing the interaction energies of the docked compound with those of the crystal structure, new interactions as well as conserved ones could be visualized. Figure 10 in the Results and Discussion section shows an example of such a comparison. For a more detailed description of the energy calculations see ref 50.

Table 1

(a) 1GZ8 (1 Anchor Point)

% of ranked database	$KA_{\%}$[a]	$NC_{\%}$[b]	KA_{total}[c]	NC_{total}[d]	RF[f]
1	4	787	11	78,670	36
2	4	1573	11	78,670	18
10	10	7867	11	78,670	9

(b) 1URW (2 Anchor Points)

% of ranked database	$KA_{\%}$[a]	$NC_{\%}$[b]	KA_{total}[c]	NC_{total}[e]	RF[f]
1	18	334	29	33,376	62
2	20	668	29	33,376	34
10	21	3338	29	33,376	7

[a] Number of known actives recovered in x % of the database. [b] Number of compounds in x % of the database. [c] Total number of known actives in the database. [d] Total number of compounds in the database with one anchor point. [e] Total number of compounds in the database with two anchor points. [f] The recovery factor.

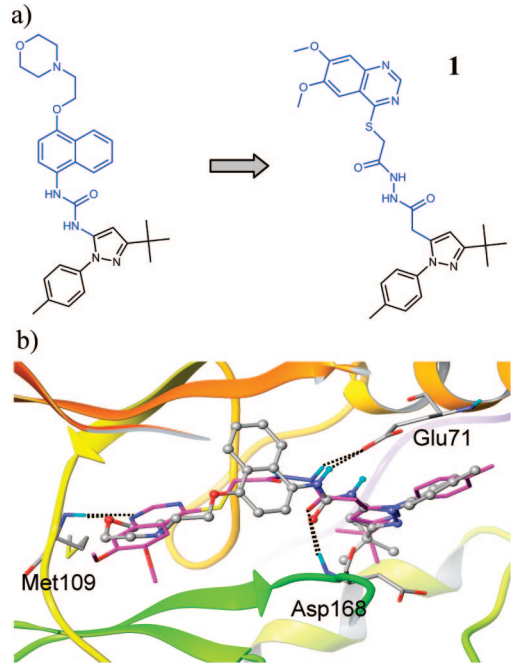

Figure 7. (a) The new scaffold **1** obtained by a SHOP search with the 1KV2 receptor and the one anchor point scaffold as query. The selected one anchor point query structure of 1KV2 and the new scaffold from the database are illustrated in blue. (b) In gray is BIRB 796 from the 1KV2 X-ray structure, and in magenta the docked pose of **1** is illustrated.

RESULTS AND DISCUSSION

CDK2 Recovery. To evaluate the receptor-based scaffold hopping procedure, a database containing 124.317 scaffolds, seeded with 47 known actives, was searched using a one and a two anchor point query (Figure 6) obtained from the CDK2 structures 1GZ8 and 1URW, respectively.

For the tested queries, SHOP showed an encouraging ability to recover structurally diverse known active scaffolds. Figure 6 shows the enrichment curves. The recovery factors are presented in Table 1a,b, and show that the improvement in recovery of known actives compared to random is high already among the scaffolds that ranked at the top 1% of the database. In the top 1% of the database, the recovery factor was 36 for the one anchor point scaffold, while the recovery was 62-fold compared to random for the two anchor

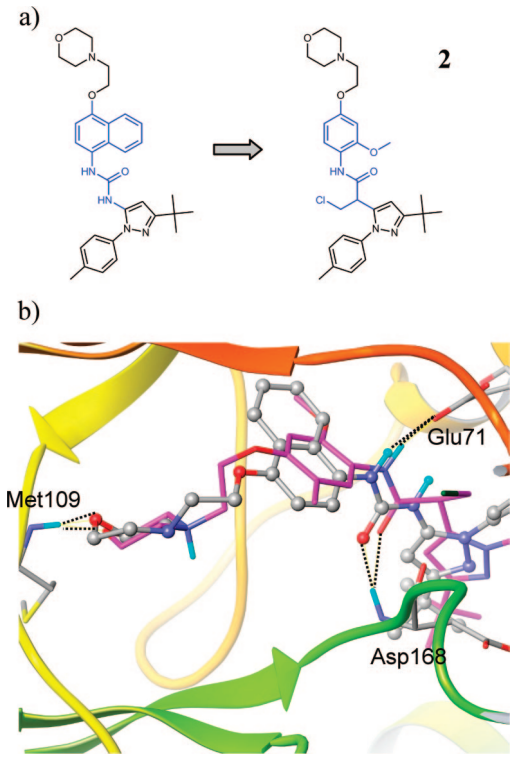

Figure 8. (a) The new scaffold **2** obtained by a SHOP search with the 1KV2 receptor and the two anchor point scaffold as queries. The selected two anchor point query structure of 1KV2 and the new scaffold from the database are depicted in blue. (b) BIRB 796 from the 1KV2 X-ray structure is illustrated in gray and the docked pose of **2** in magenta.

point scaffold. When looking at 10% of the database, the recovery was greater for the one anchor point scaffold since 10 of the 11 scaffolds were recovered. For the two anchor point scaffold query 21 of 29 scaffolds were recovered in the top 10% of the two anchor point bin. These numbers show that the SHOP descriptors and the way they are compared are successful in finding already known active CDK2 scaffolds in their bioactive conformation. This is the case even when the geometric descriptors are not possible to include as is the case for one anchor point scaffolds.

p38 Case Studies. The p38 study was conducted using one, two, and three anchor point queries obtained from four X-ray complexes. In the similarity calculation the weight for the negative probe was set to 0.0 to improve results. Otherwise carboxylic acids were dominating the results due to the electrostatics of Lys53. The results of the search after the postprocessing procedure using Glide XP for docking the top 100 hits are presented in Table 2. The final column of Table 2 shows the number of database scaffolds among the top 100 after the postfiltering procedure i.e. they were docked with the substituents with an rmsd within 3 Å from the X-ray structure and had an interaction with Met109 with an interaction energy ≤ -4 kcal/mol. The numbers range from 3 to 29 new scaffold suggestions. One example of scaffold hopping will be illustrated in detail for each of the p38 query scaffolds. The new scaffold suggestions are all novel compared to the query scaffolds. In some cases, the new scaffolds contain slightly different structures, while in most cases the new scaffolds were significantly different in their structural composition. When examining the results it is important to focus on SHOP as a generator of ideas for new scaffolds that are not obvious substitutes of the query scaffold. These may subsequently need further optimization.

The new compounds were docked into the query receptors to investigate whether they would fit into the receptor they were predicted to bind to. The current docking programs and their scoring functions cannot replace synthesis and pharmacological testing of compounds. However, they do give a good idea of whether or not a ligand could fit into a receptor. Furthermore, it should be noted that the SHOP descriptors do not penalize steric clashes with the receptor, which the postdocking procedure accounts for.

Allosteric Site. When a lead structure is already patented by another source, substitution of several different fragments of the lead may be investigated. Three different scaffolds were defined from 1KV2 to illustrate this approach of developing new p38 inhibitors (Figure 5).

1KV2, 1 Anchor Point. Four new scaffolds remained after the postfiltering procedure. Compound **1**, the highest ranked compound for both the 1 Å and 2 Å cutoff distance, is shown in Figure 7. The morpholino head of the query scaffold, which accepts a hydrogen bond from the backbone NH of Met109, was substituted by a 6,7-dimethoxyquinazoline, a well-known kinase hinge-binding motif.[51−55] The quinazoline is known to bind to p38 in the orientation predicted by the docking study with the N1 accepting a hydrogen bond from the Met109 backbone NH. The 1DI9[52] and 2BAK[55] X-ray structures from the PDB contain quinazoline ligands. Here Thr106 furthermore donates a hydrogen bond to N3 of the quinazoline, in 1DI9 via a water molecule. Due to the orientation of the Thr106 in the 1KV2 crystal structure this does not occur in the docked pose of **1**. Moreover, in both X-ray structures a polar interaction is observed between the quinazoline C2 and the carbonyl of His107. Due to a slight conformational difference in the hinge region of 1KV2 this interaction is weak (distance 3.5Å) in the docked pose of **1**. The substitution of the morpholine with a quinazoline is not obvious and is a good example of the strength of the method. The valuable 3D information from the protein allowed for this bioisosteric replacement where structure, shape, and interaction pattern were quite different from the original morpholino-motif. A hydrophobic motif interacting in the hydrophobic region I was not found in **1** but was found in other suggested scaffolds. Finally, the urea motif was replaced by a diaryl hydrazine in **1**. The hydrogen bonds formed by the query scaffold urea with Glu71 and Asp168 of the p38 receptor are both reproduced by an amide in the predicted binding mode of **1**. The tert-butyl and tolyl groups are making the same hydrophobic interactions as in the native 1KV2 X-ray structure.

1KV2, 2 Anchor Points. In this search, compound **2** was the eighth and 14th ranked scaffold suggestion for 1 Å and 2 Å cut out distances, respectively (Figure 8). Eight new scaffolds were suggested by SHOP that could be docked according to the criteria described above. The morpholino ether oxygen of **2** is predicted to make the same hydrogen bond with Met109 as BIRB 796, and a methoxyphenyl group replaces the naphthyl fragment in the hydrophobic region I (Figure 8). As for **1,** the urea motif is substituted by an amide forming the same hydrogen bonds as seen in the 1KV2 X-ray structure. Although, the aromatic moiety in the hydrophobic pocket I is different, the connectivity of the amide and morpholino substituents on the phenyl ring is the same as in

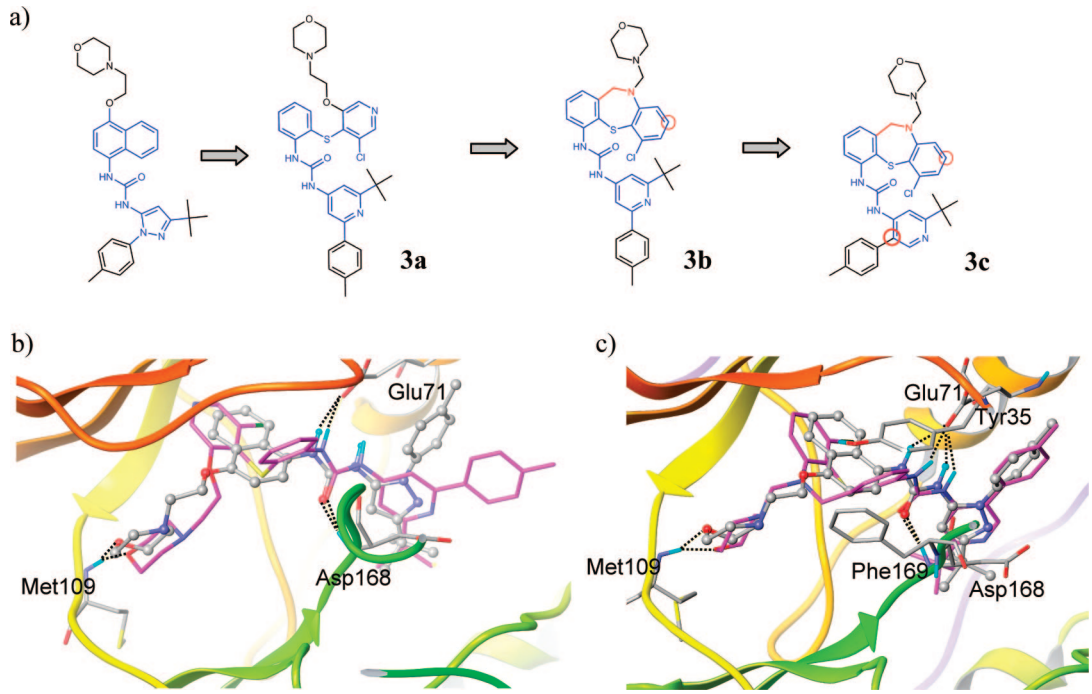

Figure 9. (a) BIRB 796 and the new compounds **3a**, **3b**, and **3c**.The three anchor point query scaffold, the new database scaffold, and the modifications of this are illustrated in blue. Red markings illustrate manual optimization. The docked poses of **3a** (b) and **3c** (c) are illustrated in magenta sticks, while the X-ray structure of BIRB in the p38 receptor is showed in gray ball and sticks.

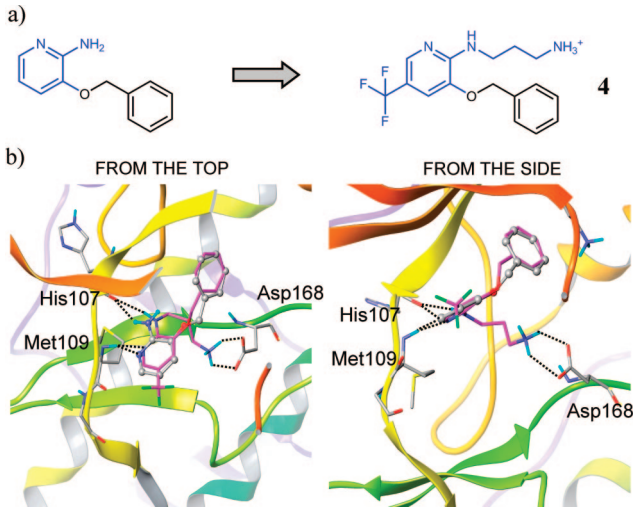

Figure 10. (a) The one anchor point query scaffold from the 1W7H and the new scaffold from the database are depicted in blue. (b) The docked pose of **4** is illustrated in magenta sticks, while the X-ray ligand is shown in gray ball and sticks.

Table 2. Number of Database Scaffolds from Each Search That Passed the Postprocessing Steps

query (anchor points)	cut-off distance (Å)	compounds in top 100[a]	rms ≤ 3 Å	E_{Met109} ≤ −4 kcal/mol[b]
1KV2 (1)	1	24	6	4
	2	19	5	3
1KV2 (2)	1	32	6	5
	2	34	10	8
1KV2 (3)	1	31	5	3
	2	37	6	5
1W7H (1)	1	38	34	29
	2	25	21	16
1YQJ (2)	1	27	11	11
	2	25	11	11
1BMK (3)	1	43	5	5
	2	44	4	4

[a] The number of compounds among the top 100 corrected for the presence of multiple conformers. [b] The number of compounds with rms ≤ 3 Å and E_{Met109} ≤ −4 kcal/mol.

1KV2. In the predicted binding mode of **2,** the tert-butyl and tolyl fragments are both interacting as in the 1KV2 structure.

1KV2, 3 Anchor Points. Compound **3a** (Figure 9) is the highest ranked new allosteric three anchor point scaffold suggested by SHOP. The naphthyl fragment interacting in the hydrophobic pocket I is replaced by a 3-chloro-4-(phenylthio)pyridine which is another example of a nonobvious substitution. The predicted binding interactions are new, and one of them is not observed in any currently published X-ray structure of p38 (Figure 9). The chloropyridine ring is predicted to bind in the hydrophobic region I, and the phenyl ring is positioned in a hydrophobic region formed between the Phe169 and Tyr35 (Figure 9). The urea motif is conserved in the new scaffold, and the imidazole is replaced by a pyridine. The morpholino and the tert-butyl substituents are located in their original positions, but the tolyl substituent is directed toward the solvent.

Recalling the purpose of SHOP is to find ideas for new bioisosteric scaffold replacements and then further optimize them, further development of compound **3a** was attempted by increasing the structural rigidity of the new scaffold as well as improving the ligand−protein complementarities. The pyridine in the hydrophobic region I was converted into a phenyl ring since the nitrogen points straight into the hydrophobic pocket I. The two phenyl rings were then connected and converted into a tricyclic ring system with a seven-membered ring between the phenyl rings to obtain **3b**.

Since docking of **3b** revealed that the tolyl substituent was directed out toward the solvent instead of having favorable contacts with the carbon chains of Glu71, Arg67, and Arg70 like the BIRB 796 X-ray structure, the tolyl ring was moved

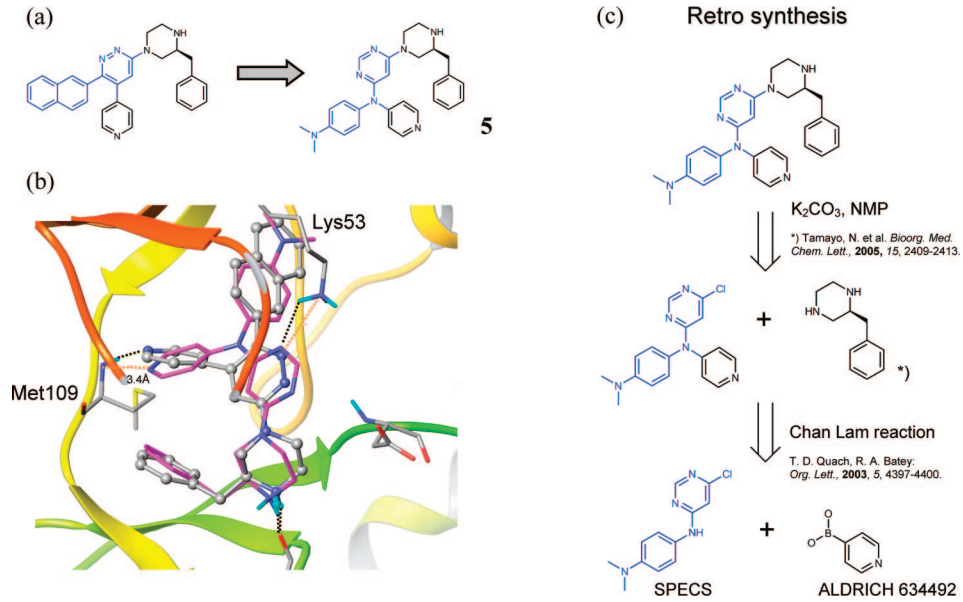

Figure 11. The two anchor point query scaffold from 1YQJ and the new database scaffold of **5** are illustrated in blue (a). (b) The docked pose of **5** is illustrated in magenta sticks, while the X-ray ligand is showed in gray ball and sticks. A retrosynthesis was designed for **5** (c).

from the 6-position to the 5-position of the pyridine linker to obtain **3c**. Pyridine is a larger linker than imidazole, and steric hindrance was observed for the tert-butyl and tolyl groups. The kinase binding sites are known to be flexible, and probably the backbone of a loop or just side chains could move to better accommodate **3c**. Thus, the Induced Fit Docking[56,57] methodology in GLIDE was used to investigate whether movements in the hydrophobic region III or in the side chains surrounding the tolyl substituent could better accommodate the enlargement of the linker. An overall movement of 0.9 Å of residues within 5 Å from the ligand occurred to better accommodate **3c**. The result was a five unit increase of the XP docking score of **3c** compared to **3b** and an increase of four units compared to BIRB 796 which is a good indication that **3c** could bind well to p38.

The ATP site. For the three ATP competitive inhibitors, only one scaffold has been defined for each inhibitor (Figure 5).

1W7H. The 1W7H complex contains the inhibitor 3-(benzyloxy)pyridin-2-amine which was originally identified as a p38 binding fragment from an X-ray screen made by Astex Technology.[43]

The inhibitor has very low in vitro affinity but was selected as a hit by Astex Technology due to the well defined binding mode and the potential for optimization of the small compound.[43] It was further developed into potent p38 inhibitors. The reason for including the complex as a query in the present study was to investigate the ability of the SHOP method to discover new interactions with the receptor.

The 1W7H searches resulted in the highest number of new scaffolds within the top 100 passing the postprocessing filters (Table 2). Compound **4** (Figure 10) was the highest ranked new scaffold from the 1W7H complex searches. The query scaffold was conserved within **4** but additions to the scaffold were observed. Based on the interaction profile information, a trifluoro-methyl substituent was included in the 5-position of the pyridine ring and a 3-amino-propyl substituent was connected to the 2-amino group attached to the pyridine. All original interactions of the 1W7H ligand are conserved. The polar trifluoro-methyl substituent is directed toward the solvent. The amino-propyl group is able to form a salt bridge with Asp168. Again, this is an example of new interaction possibilities being identified in the receptor. Indeed, looking at a plot of the interaction energies between each amino acid in the binding site with **4** vs interactions with the 1W7H ligand, it is found that all interactions except the interaction with Asp168 are conserved (Figure 10). The docking score of **4** was increased by two units compared to the 1W7H ligand.

1YQJ. The selected scaffold includes the naphthyl fragment interacting in the hydrophobic pocket I (Figure 5). The pyridazine fragment acts as a linker between the naphthyl and the pyridine moieties interacting with the hinge Met109 as well as forming a neutral-charged hydrogen bond with Lys53. The remaining substituents were attached to the new scaffolds suggested by SHOP.

Compound **5** (Figure 11) was ranked fourth (1 Å cutoff distance) and fifth (2 Å cutoff distance) in the query for new scaffolds able to substitute the 1YQJ query scaffold. The scaffold of **5** contains a N^1,N^1-dimethyl-N^4-(pyrimidin-4-yl)benzene-1,4-diamine, the pyrimidine ring substituting the pyridazine ring and the N,N-dimethylaniline substituting the naphthyl in the hydrophobic pocket I. A hydrogen bond between Lys53 and a pyrimidine nitrogen is predicted similar to the Lys53-pyridazine interaction in the query. The new scaffold in **5** introduces a different connectivity of the pyrimidine compared to that of the pyridazine. A replacement of a pyridazine by a pyrimidine may be considered trivial, but the added change in substitution pattern increases the complexity of the change. The pyrimidine ring is 4,6-disubstituted, while the query pyridazine ring is 3,4,6-trisubstituted with the hinge binding pyridyl ring directly attached to the ring. This pyridine side chain is connected to the amine connecting the two aromatic rings in scaffold **5** leading to a small change in the angle of the necessary hydrogen bond with the hinge Met109.

The angular change resulted in a loss of the hydrogen bond. In general the active sites of the kinases are known to

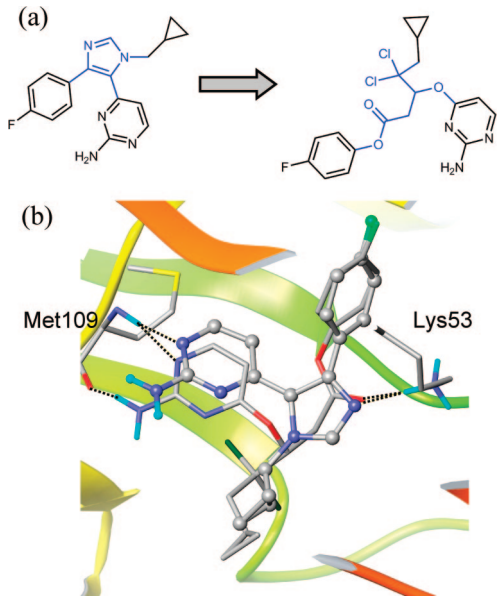

Figure 12. (a) The three anchor point query scaffold of 1BMK and the new database scaffold are illustrated in blue. (b) The docked pose of **6** is shown in sticks, while the X-ray structure is depicted in ball and sticks.

be flexible, and thus the hydrogen bond might be obtained in a complex of p38 with **5**.

The Virtual Reaction utility program, which has been used to build the databases in this study, is constructed in such a way that it is possible to back track the reaction(s) used to construct each scaffold. Although, there is no guarantee that a scaffold in the database can actually be synthesized, there is synthetic reasoning in the way they are constructed. Coupling known reactions and purchasable reactants in the construction of the scaffolds facilitates the synthesis of the scaffold and the final compound. Making a database of synthetically feasible scaffold, where also the attachment of substituents should be potentially possible, is not a simple task. The Virtual Reaction utility program is constructed in such a way that a chemical 'handle' at the substituents is ensured, in the shape of the fragments participating in each reaction (an aldehyde and a β-keto ester in the Biginelli reaction in Figure 4). However, the availability of these reagents is not assured and must be considered subsequently. With the purpose of the Virtual Reaction utility program in mind a retrosynthetic scheme was attempted for compound **5** (Figure 11).

1BMK. The chosen imidazole scaffold of the 1BMK ligand acts as a linker between the three substituents that were removed from the query scaffold and reattached to the new scaffolds.

From a drug discovery point of view the best ranked scaffold of the 1BMK search **6** was not a perfect new scaffold due to its flexibility (Figure 12). Nevertheless, the predicted binding mode gave inspiration for how to bioisosterically replace the imidazole N with an ester carbonyl from the pentanoate scaffold of **6** which has an entirely different structure than that of the 1BMK scaffold.

CONCLUSION

High recovery factors were obtained with a test set of 42 structurally divergent CDK2 scaffolds showing that for this target receptor-based SHOP is highly successful. In the first 1% of the ranked database, the recovery rate was increased 36- and 62-fold compared to random for the 1 anchor point scaffold and the 2 anchor point scaffold, respectively.

The combination of receptor-based scaffold hopping with SHOP followed by a docking approach resulted in the identification of new and structurally different ligand proposals for the p38 MAP kinase. However, in one case (1YQJ) the best new scaffold was quite flexible showing that the success also depends on the database in use. In several cases, the new scaffolds interacted differently with the receptor, highlighting potential routes for lead optimization. This information is valuable and of great use in structure-based ligand design, making receptor-based SHOP an important new tool in drug design.

ACKNOWLEDGMENT

Drug Research Academy and LEO Pharma A/S are gratefully acknowledged for supporting the study financially. Furthermore, Thomas Balle is acknowledged for his thorough proofreading and feedback to this article.

Supporting Information Available: List of the CDK2 scaffolds included in the recovery study. This material is available free of charge via the Internet at http://pubs.acs.org.

REFERENCES AND NOTES

(1) Friesner, R. A.; Banks, J. L.; Murphy, R. B.; Halgren, T. A.; Klicic, J. J.; Mainz, D. T.; Repasky, M. P.; Knoll, E. H.; Shelley, M.; Perry, J. K.; Shaw, D. E.; Francis, P.; Shenkin, P. S. Glide: a new approach for rapid, accurate docking and scoring. 1. Method and assessment of docking accuracy. *J. Med. Chem.* **2004**, *47*, 1739–1749.
(2) Halgren, T. A.; Murphy, R. B.; Friesner, R. A.; Beard, H. S.; Frye, L. L.; Pollard, W. T.; Banks, J. L. Glide: a new approach for rapid, accurate docking and scoring. 2. Enrichment factors in database screening. *J. Med. Chem.* **2004**, *47*, 1750–1759.
(3) McInnes, C. Improved lead-finding for kinase targets using high-throughput docking. *Curr. Opin. Drug Discovery Dev.* **2006**, *9*, 339–347.
(4) Warren, G. L.; Andrews, C. W.; Capelli, A. M.; Clarke, B.; LaLonde, J.; Lambert, M. H.; Lindvall, M.; Nevins, N.; Semus, S. F.; Senger, S.; Tedesco, G.; Wall, I. D.; Woolven, J. M.; Peishoff, C. E.; Head, M. S. A critical assessment of docking programs and scoring functions. *J. Med. Chem.* **2006**, *49*, 5912–5931.
(5) Güner, O. F. History and evolution of the pharmacophore concept in computer-aided drug design. *Curr. Top. Med. Chem.* **2002**, *2*, 1321–1332.
(6) Verdonk, M. L.; Hartshorn, M. J. Structure-guided fragment screening for lead discovery. *Curr. Opin. Drug Discovery Devl.* **2004**, *7*, 404–410.
(7) Honma, T. Recent advances in de novo design strategy for practical lead identification. *Med. Res. Rev.* **2003**, *23*, 606–632.
(8) Degen, J.; Rarey, M. FlexNovo: structure-based searching in large fragment spaces. *ChemMedChem* **2006**, *1*, 854–868.
(9) Miranker, A.; Karplus, M. Functionality maps of binding sites: a multiple copy simultaneous search method. *Proteins* **1991**, *11*, 29–34.
(10) Schneider, G.; Lee, M. L.; Stahl, M.; Schneider, P. De novo design of molecular architectures by evolutionary assembly of drug-derived building blocks. *J. Comput.-Aided Mol. Des.* **2000**, *14*, 487–494.
(11) Lauri, G.; Bartlett, P. A. CAVEAT: a program to facilitate the design of organic molecules. *J. Comput.-Aided. Mol. Des.* **1994**, *8*, 51–66.
(12) Schneider, G.; Neidhart, W.; Giller, T.; Schmid, G. "Scaffold-Hopping" by Topological Pharmacophore Search: A Contribution to Virtual Screening. *Angew. Chem., Int. Ed. Engl.* **1999**, *38*, 2894–2896.
(13) Naerum, L.; Norskov-Lauritsen, L.; Olesen, P. H. Scaffold hopping and optimization towards libraries of glycogen synthase kinase-3 inhibitors. *Bioorg. Med. Chem. Lett.* **2002**, *12*, 1525–1528.
(14) Abolmaali, S. F.; Ostermann, C.; Zell, A. The Compressed Feature Matrix--a novel descriptor for adaptive similarity search. *J. Mol. Model. (Online)* **2003**, *9*, 66–75.

(15) Raymond, J. W.; Willett, P. Similarity searching in databases of flexible 3D structures using smoothed bounded distance matrices. *J. Chem. Inf. Comput. Sci.* **2003**, *43*, 908–916.
(16) Jenkins, J. L.; Glick, M.; Davies, J. W. A 3D similarity method for scaffold hopping from known drugs or natural ligands to new chemotypes. *J. Med. Chem.* **2004**, *47*, 6144–6159.
(17) Stiefl, N.; Watson, I. A.; Baumann, K.; Zaliani, A. ErG: 2D pharmacophore descriptions for scaffold hopping. *J. Chem. Inf. Model.* **2006**, *46*, 208–220.
(18) Stiefl, N.; Zaliani, A. A knowledge-based weighting approach to ligand-based virtual screening. *J. Chem. Inf. Model.* **2006**, *46*, 587–596.
(19) Zhang, Q.; Muegge, I. Scaffold hopping through virtual screening using 2D and 3D similarity descriptors: ranking, voting, and consensus scoring. *J. Med. Chem.* **2006**, *49*, 1536–1548.
(20) Maass, P.; Schulz-Gasch, T.; Stahl, M.; Rarey, M. Recore: a fast and versatile method for scaffold hopping based on small molecule crystal structure conformations. *J. Chem. Inf. Model.* **2007**, *47*, 390–399.
(21) Bergmann, R.; Linusson, A.; Zamora, I. SHOP: Scaffold HOPping by GRID-Based Similarity Searches. *J. Med. Chem.* **2007**, *50*, 2708–2717.
(22) *COMBIGLIDE*; Schrödinger, LLC: New York, NY, U.S.A., **2007**.
(23) Smith, K.; Masek, B.; Clark, R.; Mansley, T.; Abrahamian, E.; Nagy, S. EAI-TupletScore, a Pharmacophore and Shape Driven Ligand-Based Denovo Design Program. Submitted to *J. Chem. Inf. Model*.
(24) *GRID v. 22*; Molecular Discovery Ltd.: 215 Marsh Road, HA5 5NE Pinner, Middlesex, U.K., 2004.
(25) Goodford, P. J. A computational procedure for determining energetically favourable binding sites on biologically important macromolecules. *J. Med. Chem.* **1985**, *28*, 849–857.
(26) Pargellis, C.; Tong, L.; Churchill, L.; Cirillo, P. F.; Gilmore, T.; Graham, A. G.; Grob, P. M.; Hickey, E. R.; Moss, N.; Pav, S.; Regan, J. Inhibition of p38 MAP kinase by utilizing a novel allosteric binding site. *Nat. Struct. Biol.* **2002**, *9*, 268–272.
(27) Brown, N. R.; Noble, M. E.; Lawrie, A. M.; Morris, M. C.; Tunnah, P.; Divita, G.; Johnson, L. N.; Endicott, J. A. Effects of phosphorylation of threonine 160 on cyclin-dependent kinase 2 structure and activity. *J. Biol. Chem.* **1999**, *274*, 8746–8756.
(28) Ohren, J. F.; Chen, H.; Pavlovsky, A.; Whitehead, C.; Zhang, E.; Kuffa, P.; Yan, C.; McConnell, P.; Spessard, C.; Banotai, C.; Mueller, W. T.; Delaney, A.; Omer, C.; Sebolt-Leopold, J.; Dudley, D. T.; Leung, I. K.; Flamme, C.; Warmus, J.; Kaufman, M.; Barrett, S.; Tecle, H.; Hasemann, C. A. Structures of human MAP kinase kinase 1 (MEK1) and MEK2 describe novel noncompetitive kinase inhibition. *Nat. Struct. Mol. Biol.* **2004**, *11*, 1192–1197.
(29) Pastor, M.; Cruciani, G.; McLay, I.; Pickett, S.; Clementi, S. GRid-INdependent descriptors (GRIND): a novel class of alignment-independent three-dimensional molecular descriptors. *J. Med. Chem.* **2000**, *43*, 3233–3243.
(30) Fontaine, F.; Pastor, M.; Zamora, I.; Sanz, F. Anchor-GRIND: filling the gap between standard 3D QSAR and the GRid-INdependent descriptors. *J. Med. Chem.* **2005**, *48*, 2687–2694.
(31) Kastenholz, M. A.; Pastor, M.; Cruciani, G.; Haaksma, E. E.; Fox, T. GRID/CPCA: a new computational tool to design selective ligands. *J. Med. Chem.* **2000**, *43*, 3033–3044.
(32) Carbo, R.; Leyda, L.; Arnau, M. How similar is a molecule to another? An electron density measure of similarity between two molecular structures. *Int. J. Quantum Chem.* **1980**, *17*, 1185–1189.
(33) Biginelli, P. Aldehyde-uridic derivative of ether acetyl and diossal-acetic. *Gazz. Chim. Ital.* **1893**, *23*, 360–416.
(34) Baroni, M.; Cruciani, G.; Sciabola, S.; Perruccio, F.; Mason, J. S. A common reference framework for analyzing/comparing proteins and ligands. Fingerprints for Ligands and Proteins (FLAP): theory and application. *J. Chem. Inf. Model.* **2007**, *47*, 279–294.
(35) Maybridge. http://www.maybridge.com (accessed June 15, 2005).
(36) Specs. http://www.specs.net (accessed June 15, 2005).
(37) Research Collaboratory for Structural Bioinformatics (RCSB) Protein Data Bank. http://www.rcsb.org/pdb/ (accessed July 20, 2005).
(38) Berman, H. M.; Westbrook, J.; Feng, Z.; Gilliland, G.; Bhat, T. N.; Weissig, H.; Shindyalov, I. N.; Bourne, P. E. The Protein Data Bank. *Nucleic Acids Res.* **2000**, *28*, 235–242.
(39) *MAESTRO v. 7.5*; Schrödinger LLC: New York, NY, U.S.A., **2006**.
(40) Lovell, S. C.; Davis, I. W.; Arendall, W. B., III; de Bakker, P. I.; Word, J. M.; Prisant, M. G.; Richardson, J. S.; Richardson, D. C. Structure validation by Calpha geometry: phi,psi and Cbeta deviation. *Proteins* **2003**, *50*, 437–450.
(41) Sali, A.; Blundell, T. L. Comparative protein modelling by satisfaction of spatial restraints. *J. Mol. Biol.* **1993**, *234*, 779–815.
(42) Nagar, B.; Bornmann, W. G.; Pellicena, P.; Schindler, T.; Veach, D. R.; Miller, W. T.; Clarkson, B.; Kuriyan, J. Crystal structures of the kinase domain of c-Abl in complex with the small molecule inhibitors PD173955 and imatinib (STI-571). *Cancer Res.* **2002**, *62*, 4236–4243.
(43) Gill, A. L.; Frederickson, M.; Cleasby, A.; Woodhead, S. J.; Carr, M. G.; Woodhead, A. J.; Walker, M. T.; Congreve, M. S.; Devine, L. A.; Tisi, D.; O'Reilly, M.; Seavers, L. C.; Davis, D. J.; Curry, J.; Anthony, R.; Padova, A.; Murray, C. W.; Carr, R. A.; Jhoti, H. Identification of novel p38alpha MAP kinase inhibitors using fragment-based lead generation. *J. Med. Chem.* **2005**, *48*, 414–426.
(44) Tamayo, N.; Liao, L.; Goldberg, M.; Powers, D.; Tudor, Y. Y.; Yu, V.; Wong, L. M.; Henkle, B.; Middleton, S.; Syed, R.; Harvey, T.; Jang, G.; Hungate, R.; Dominguez, C. Design and synthesis of potent pyridazine inhibitors of p38 MAP kinase. *Bioorg. Med. Chem. Lett.* **2005**, *15*, 2409–2413.
(45) Wang, Z.; Canagarajah, B. J.; Boehm, J. C.; Kassisa, S.; Cobb, M. H.; Young, P. R.; Abdel-Meguid, S.; Adams, J. L.; Goldsmith, E. J. Structural basis of inhibitor selectivity in MAP kinases. *Structure* **1998**, *6*, 1117–1128.
(46) *LIGPREP v. 2.0*; Schrödinger, LLC: New York, NY, U.S.A., 2005.
(47) *GLIDE v. 4.0*; Schrödinger, LLC: New York, NY, U.S.A., 2005.
(48) Friesner, R. A.; Murphy, R. B.; Repasky, M. P.; Frye, L. L.; Greenwood, J. R.; Halgren, T. A.; Sanschagrin, P. C.; Mainz, D. T. Extra precision glide: docking and scoring incorporating a model of hydrophobic enclosure for protein-ligand complexes. *J. Med. Chem.* **2006**, *49*, 6177–6196.
(49) *GRID manual*; Molecular Discovery Ltd.: 215 Marsh Road, 1st Floor, HA5 5NE, Pinner, Middlesex, U.K., 2004. http://www.moldiscovery.com/docs/grid/ (accessed September 3, 2008).
(50) Kjellander, B.; Masimirembwa, C. M.; Zamora, I. Exploration of enzyme-ligand interactions in CYP2D6 & 3A4 homology models and crystal structures using a novel computational approach. *J. Chem. Inf. Model.* **2007**, *47*, 1234–1247.
(51) Moyer, J. D.; Barbacci, E. G.; Iwata, K. K.; Arnold, L.; Boman, B.; Cunningham, A.; DiOrio, C.; Doty, J.; Morin, M. J.; Moyer, M. P.; Neveu, M.; Pollack, V. A.; Pustilnik, L. R.; Reynolds, M. M.; Sloan, D.; Theleman, A.; Miller, P. Induction of apoptosis and cell cycle arrest by CP-358,774, an inhibitor of epidermal growth factor receptor tyrosine kinase. *Cancer Res.* **1997**, *57*, 4838–4848.
(52) Shewchuk, L.; Hassell, A.; Wisely, B.; Rocque, W.; Holmes, W.; Veal, J.; Kuyper, L. F. Binding mode of the 4-anilinoquinazoline class of protein kinase inhibitor: X-ray crystallographic studies of 4-anilinoquinazolines bound to cyclin-dependent kinase 2 and p38 kinase. *J. Med. Chem.* **2000**, *43*, 133–138.
(53) Barker, A. J.; Gibson, K. H.; Grundy, W.; Godfrey, A. A.; Barlow, J. J.; Healy, M. P.; Woodburn, J. R.; Ashton, S. E.; Curry, B. J.; Scarlett, L.; Henthorn, L.; Richards, L. Studies leading to the identification of ZD1839 (IRESSA): an orally active, selective epidermal growth factor receptor tyrosine kinase inhibitor targeted to the treatment of cancer. *Bioorg. Med. Chem. Lett.* **2001**, *11*, 1911–1914.
(54) Cumming, J. G.; McKenzie, C. L.; Bowden, S. G.; Campbell, D.; Masters, D. J.; Breed, J.; Jewsbury, P. J. Novel, potent and selective anilinoquinazoline and anilinopyrimidine inhibitors of p38 MAP kinase. *Bioorg. Med. Chem. Lett.* **2004**, *14*, 5389–5394.
(55) Sullivan, J. E.; Holdgate, G. A.; Campbell, D.; Timms, D.; Gerhardt, S.; Breed, J.; Breeze, A. L.; Bermingham, A.; Pauptit, R. A.; Norman, R. A.; Embrey, K. J.; Read, J.; VanScyoc, W. S.; Ward, W. H. Prevention of MKK6-dependent activation by binding to p38alpha MAP kinase. *Biochemistry* **2005**, *44*, 16475–16490.
(56) Schrödinger Suite 2006 Induced Fit Docking Protocol. *GLIDE v. 4.0*; Schrödinger, LLC: New York, NY, U.S.A., 2005. *PRIME v. 1.5*; Schrödinger, LLC: New York, NY, U.S.A., **2005**.
(57) Sherman, W.; Day, T.; Jacobson, M. P.; Friesner, R. A.; Farid, R. Novel procedure for modeling ligand/receptor induced fit effects. *J. Med. Chem.* **2006**, *49*, 534–553.

CI800391V